# A Variational Link of Marking to Color for Color Printing Technologies: The Color Gain Matrix for the Simple Estimation of Print to Print Variation

*Michael Sanchez, DocuSP Controller Color Science Team, Xerox;*
*Martin Maltz, Xerox Innovation Group, Xerox, Webster, New York, USA*

## Abstract

Profitable print image reproduction is highly dependent upon print to print and between print run variability. This paper presents methods extracted from process control technology and linear systems to provide a powerful, yet simple, method of estimating printing color white noise (print to print variability). These methods are then utilized to estimate mean color white noise (in $\Delta E_{ab}$), along the neutral axes for both the CGATS SWOP TR001 and the CGATS SWOP TR004 offset press standards. Given a known uncertainty in separation marking, local color white noise is immediately available. Both correlated and uncorrelated variation in c,m,y are considered.

Total color error emanating from correlated fluctuations in c,m,y and uncorrelated fluctuations in c,m,y are computed and presented. Contrary to many natural systems where all variables are subject to positive or zero variability, uncorrelated error exceeds correlated error.

Partial differential linearization methods are utilized to quantitatively compute color gain, and color error, associated with forced changes in marking digital count (uncertainty in marking). These linearization methods are applied along the neutral axes of the SWOP TR004 and SWOP TR001 four color presses. From each linearization term a gain matrix associated with each separation can be extracted. This gain matrix provides, at a glance, the variational structure of color for changes in marking. Having constructed a Jacobian, relating L*a*b* to variational terms in c,m,y, the overall Euclidean, correlated and uncorrelated, color error can be computed for a given local marking fluctuation in c,m,y.

These methods, commonly utilized to estimate local control point stability of process control systems in the process industry and electronics, provide simple and powerful methods for estimating color stability around local points in color space for digital printing. Given the importance of estimating print to print variability for given colorant and halftone, these methods are powerful and do not require the print and measurement of thousands of prints to extract.

The neutral axes of a c,m,y color space employs all three separations along a critical line where the eye is most sensitive to color variation. Hence, it is this axis for which the techniques developed are applied. Color gain is computed in increments of 5 L*, beginning at L*=95 along the neutral axes of the SWOP TR001 and SWOP TR004 specification.

A comprehensive comparison of the neutral axes of both TR001 and TR004 specifications is a byproduct of the development of color gain.

## Introduction

In complex process control systems it is common to use either simple phenomenological models or carefully collected data to estimate response around a point. From this response the open loop gain between an input variable and an output variable can be estimated for that localized region.[1,2] This open loop gain is critical to the design of controls and to the assessment of variability at sampling, data acquisition or process control resolution.[3]

Linearization methods, for complex systems, can be utilized in the assessment of color gain and color variability in specific regions of color space. In the application of these methods the input variable is digital count (which drives the halftone laydown for digital printing) and the output variable of keen interest is color (where color can be represented by any color space....as complex or as simple as necessary for the application).

## Color Gain and Color Systems

Color system design requires specification and maintenance of an invariant (temporal and spatial) neutral axes[4,5,6]. A predictable and repeatable set of c, m, y, that yield neutral along a specified axis of L*, is critical for the maintenance of tone and color reproduction, print to print. For a given colorant selection and halftone selection the color gain, between digital count (directly related to halftone laydown) and a designated color space can be constructed along the neutral axis. Having constructed this gain matrix the minimum color error associated with the colorant/halftone selection can be estimated for known fluctuations in marking.

Having estimated the above gain matrix as a function of the neutral axis, it is a simple matter to extract anticipated print to print variability (or white noise) for known fluctuations in marking.

### *Development of the Color Gain Matrix: Marking to Color*

Digital printing systems, for four color systems, commonly utilize "input" data as 8 bit image content. For example, a .TIFF image created in Photoshop and saved as a raster in R, G, B 8 bit format is sent as input and rendered to 8 bit C, M, Y, K output values from 0-255. In this paper we consider that C, M, Y, K data stream, in 8 bit format, as the "input" data set.

Color outcomes associated with printing the 8 bit C, M, Y, K files are commonly measured by spectrophotometers whose spectral reflectance signal is converted to the CIE color space L*, a*, b*. This color space serves as a zero order perceptual model for human perception of color and is often utilized in process control applications where color is controlled. The CIE L*a*b* space is considered as the "output" signal for this paper. Details of the CIE L*a*b* color space may be found in Reference 7.

Further to the delivery of a time invariant neutral axis is the careful development, for all color systems, of the neutral axis formed from combinations of C, M and Y. Location of the neutral axis is critical to the calibration of offset printing systems and many other C, M, Y, K printing systems.

In general, defining the variational outcomes within color space is time and print intensive as many prints are needed to provide a statistically valid estimate.

Process control linearization methods enable variational estimates with reduced data sets.

### *Process Control to Color Variation*

In process control it is common to define a control point within a complex space and derive a linearized representation of the behavior of that control point[8].

### *Designation of the I/O Set*

Input (forcing functions) -------> **c, m, y,** (digital count): k = 0.

Output (forced functions) --------> **L*a*b*.**

Representing this I/O set in function input/output form:

$\mathbf{L^* = L^*(c_o, m_o, y_o)}$

$\mathbf{a^* = a^*(c_o, m_o, y_o)}$

$\mathbf{b^* = b^*(c_o, m_o, y_o)}$

where $c_o$, $m_o$, $y_o$ represent the c,m,y set that exists at the operating point (or the local point of interest).

Performing Taylor series expansion for each of the above we find:

$$\mathbf{L^* = L_o^* + \left[\frac{\partial L^*}{\partial c}\right]_{m,y}(c - c_o) + \left[\frac{\partial L^*}{\partial m}\right]_{c,y}(m - m_o) + \left[\frac{\partial L^*}{\partial y}\right]_{c,m}(y - y_o) + \{higher\ order\ terms\}} \quad (1)$$

$$\mathbf{a^* = a_o^* + \left[\frac{\partial a^*}{\partial c}\right]_{m,y}(c - c_o) + \left[\frac{\partial a^*}{\partial m}\right]_{c,y}(m - m_o) + \left[\frac{\partial a^*}{\partial y}\right]_{c,m}(y - y_o) + \{higher\ order\ terms\}} \quad (2)$$

$$\mathbf{b^* = b_o^* + \left[\frac{\partial b^*}{\partial c}\right]_{m,y}(c - c_o) + \left[\frac{\partial b^*}{\partial m}\right]_{c,y}(m - m_o) + \left[\frac{\partial b^*}{\partial y}\right]_{c,m}(y - y_o) + \{higher\ order\ terms\}} \quad (3)$$

$$\mathbf{L^* \cong L_o^* + \left[\frac{\partial L^*}{\partial c}\right]_{m,y}(c - c_o) + \left[\frac{\partial L^*}{\partial m}\right]_{c,y}(m - m_o) + \left[\frac{\partial L^*}{\partial y}\right]_{c,m}(y - y_o)} \quad (4)$$

For small variations in c, m, y the equations above reduce to

$$\mathbf{a^* \cong a_o^* + \left[\frac{\partial a^*}{\partial c}\right]_{m,y}(c - c_o) + \left[\frac{\partial a^*}{\partial m}\right]_{c,y}(m - m_o) + \left[\frac{\partial a^*}{\partial y}\right]_{c,m}(y - y_o)} \quad (5)$$

$$\mathbf{b^* \cong b_o^* + \left[\frac{\partial b^*}{\partial c}\right]_{m,y}(c - c_o) + \left[\frac{\partial b^*}{\partial m}\right]_{c,y}(m - m_o) + \left[\frac{\partial b^*}{\partial y}\right]_{c,m}(y - y_o)} \quad (6)$$

The above equations define the localized behavior of L*a*b* around a local operating point.

From this I/O specification of input and output data a gain matrix (Jacobian) can be constructed. This gain matrix is defined by Equation 7 from inspection of Eq. 4-6.

$$\begin{bmatrix}\Delta L\\ \Delta a\\ \Delta b\end{bmatrix}=\begin{bmatrix}\frac{\partial L^*}{\partial c} & \frac{\partial L^*}{\partial m} & \frac{\partial L^*}{\partial y}\\ \frac{\partial a^*}{\partial c} & \frac{\partial a^*}{\partial m} & \frac{\partial a^*}{\partial y}\\ \frac{\partial b^*}{\partial c} & \frac{\partial b^*}{\partial m} & \frac{\partial b^*}{\partial y}\end{bmatrix}\cdot\begin{bmatrix}\Delta c\\ \Delta m\\ \Delta y\end{bmatrix} \quad (7)$$

## Development of Euclidean Color Error: Correlated in c,m,y, Uncorrelated in L*a*b*

The total derivative of L*, associated with fluctuations in c,m,y, can be formed from:

$$\Delta L^* = \left(\frac{\partial L^*}{\partial c}\right)\cdot\Delta c + \left(\frac{\partial L^*}{\partial m}\right)\cdot\Delta m + \left(\frac{\partial L^*}{\partial y}\right)\cdot\Delta y \quad (8)$$

Likewise the total derivative of a* can be formed:

$$\Delta a^* = \left(\frac{\partial a^*}{\partial c}\right)\cdot\Delta c + \left(\frac{\partial a^*}{\partial m}\right)\cdot\Delta m + \left(\frac{\partial a^*}{\partial y}\right)\cdot\Delta y \quad (9)$$

And the total derivative of b*:

$$\Delta b^* = \left(\frac{\partial b^*}{\partial c}\right)\cdot\Delta c + \left(\frac{\partial b^*}{\partial m}\right)\cdot\Delta m + \left(\frac{\partial b^*}{\partial y}\right)\cdot\Delta y \quad (10)$$

Equations 8-10 can be combined to compute the local Euclidean color error, for correlation between c, m, y, as:

$$\Delta E_{cmy\_correlated} = \sqrt{(\Delta L^*)^2 + (\Delta a^*)^2 + (\Delta b^*)^2} \quad (11)$$

## Development of Euclidean Color Error: Uncorrelated in c,m,y, Uncorrelated in L*a*b*

Uncorrelated, in c,m,y, Euclidean color error in L*:

$$dE_{L^*} = \sqrt{\left[\left(\frac{\partial L^*}{\partial c}\right)\cdot\Delta c\right]^2 + \left[\left(\frac{\partial L^*}{\partial m}\right)\cdot\Delta m\right]^2 + \left[\left(\frac{\partial L^*}{\partial y}\right)\cdot\Delta y\right]^2} \quad (12)$$

Uncorrelated, in c,m,y, Euclidean color error in a*.

$$dE_{a^*} = \sqrt{\left[\left(\frac{\partial a^*}{\partial c}\right)\cdot\Delta c\right]^2 + \left[\left(\frac{\partial a^*}{\partial m}\right)\cdot\Delta m\right]^2 + \left[\left(\frac{\partial a^*}{\partial y}\right)\cdot\Delta y\right]^2} \quad (13)$$

Uncorrelated, in c,m,y, Euclidean color error in b*.

$$dE_{b^*} = \sqrt{\left[\left(\frac{\partial b^*}{\partial c}\right)\cdot\Delta c\right]^2 + \left[\left(\frac{\partial b^*}{\partial m}\right)\cdot\Delta m\right]^2 + \left[\left(\frac{\partial b^*}{\partial y}\right)\cdot\Delta y\right]^2} \quad (14)$$

$$\Delta E_{cmy\_uncorrelated} = \sqrt{(dE_{L^*})^2 + (dE_{a^*})^2 + (dE_{b^*})^2} \quad (15)$$

## Neutral Axes as a Critical Axes for Marking to Color Gain Estimation

Successful printing color systems provide reproducible output along a specified neutral tone reproduction curve. Indeed, the profitable utilization of printing color systems rests upon the successful extraction and reproduction of a stable neutral axes.

Further, variations in marking, translated to color, are most detectable by the human eye in the neutral region.[9]

Estimation of marking to color gain components along the neutral axis provides a quantitative window into the amplitude of color variation, for a given marking fluctuation. Larger gain components could be expected to drive larger variability in color outcomes.

Additionally, colorant selection for printing, much as process control component selection, could utilize marking to color gain as part of a larger optimization program of selection. Those colorants resulting in larger marking to color gain could be expected to provide larger print to print and run to run variability than those with smaller color to gain components. Likewise, those colorants with smaller marking to color gain might be expected to provide more stable (color) printing.

## SWOP TR001 Neutral Axes Extraction

SWOP TR001 specification IT8 data were utilized to build an accurate, forward, CMYK to L*a*b* spectral, Neugebauer, printermodel based on methods detailed by Balasubramanian[10]. A comparison of the printermodel predicted L*a*b* and actual specification data are shown in Appendix A. TR001 absolute L*a*b* data were first converted into relative colorimetric L*a*b* such that the substrate had data values L* = 100, a* = 0, b* = 0. That printermodel was then queried with a conjugate gradient search method along the c,m,y set that returns the L* = n, a* = 0, b* = 0 in L* increments of 0.25.

The neutral axes for TR001 (that c,m,y line in space which corresponds to L, 0, 0) is shown in Figure 1.

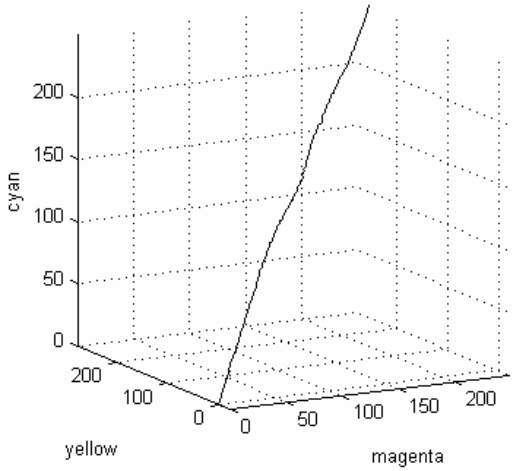


*Figure 1. TR001 c,m,y Axis Returning L*,0,0.*

TR001 neutral axis, in L* increments of 5.0, is shown.

**Table 1: TR001 Neutral Axis**

| L* | c | m | y |
|---|---|---|---|
| 95 | 14.7 | 12.3 | 13.3 |
| 90 | 29.5 | 24.4 | 26.5 |
| 85 | 45.5 | 37.7 | 39.6 |
| 80 | 60.7 | 50.5 | 53.0 |
| 75 | 75.9 | 63.3 | 65.5 |
| 70 | 91.5 | 75.0 | 79.1 |
| 65 | 107.9 | 90.4 | 92.8 |
| 60 | 125.2 | 113.3 | 114.5 |
| 55 | 142.9 | 136.3 | 136.9 |
| 50 | 165.9 | 152.8 | 155.0 |
| 45 | 187.4 | 174.2 | 174.7 |
| 40 | 206.0 | 200.2 | 202.9 |
| 35 | 227.8 | 228.3 | 231.0 |
| 30 | 250.5 | 250.3 | 255.3 |

## SWOP TR004 Neutral Axes Extraction

SWOP GATF TR004 specification IT8 data were utilized to build an accurate, forward, CMYK to L*a*b* spectral, Neugebauer, printermodel[10]. TR004 absolute L*a*b* data were first converted into relative colorimetric L*a*b* such that the substrate had data values L* = 100, a* = 0, b* = 0. That printermodel was then queried with a conjugate gradient search method along the c,m,y set that returns the L* = n, a* = 0, b* = 0 in L* increments of 0.25.

The neutral axes for TR004 (that c,m,y line in space which corresponds to L, 0, 0) is shown in Figure 2.

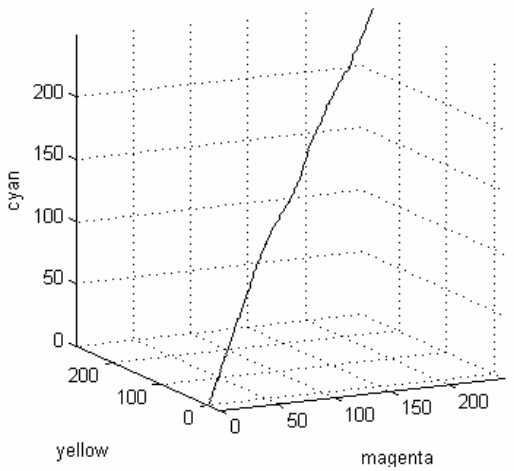


*Figure 2. TR004 c,m,y Axis Returning L*,0,0.*

**Table 2: TR004 Neutral Axis**

| L* | c | m | y |
|---|---|---|---|
| 95 | 14.5 | 11.7 | 10.9 |
| 90 | 29.9 | 22.6 | 22.1 |
| 85 | 44.5 | 34.7 | 32.4 |
| 80 | 60.3 | 46.0 | 44.2 |
| 75 | 76.0 | 57.7 | 56.3 |
| 70 | 90.7 | 69.5 | 67.0 |
| 65 | 105.5 | 82.8 | 78.3 |
| 60 | 119.9 | 97.7 | 90.0 |
| 55 | 134.7 | 116.2 | 106.3 |
| 50 | 151.2 | 133.3 | 120.8 |
| 45 | 169.9 | 150.6 | 137.4 |
| 40 | 190.5 | 167.4 | 149.1 |
| 35 | 208.8 | 189.1 | 166.4 |
| 30 | 225.3 | 221.9 | 202.3 |
| 25 | 245.7 | 246.3 | 230.3 |

## TR001 Compared with TR004 Neutral Axes.

TR001 (in blue) and TR004 (in red) are shown in Figs. 3-6. Relative to TR001, the TR004 specification results in a larger proportion of cyan relative to magenta and yellow to achieve neutral. Additionally, from Table 1 and Table 2, it can be seen that the TR004 specification results in substantially reduced L* for a given c,m,y combination (TR004 specification results in more neutral density for a given cyan laydown).

## Input Forcing Functions for Color Gain.

Extraction of the partial derivatives in Eq. 1 requires:

a. forced variations in cyan, with magenta and yellow constant.
b. forced variations in magenta, with cyan and yellow constant.
c. forced variations in yellow, with cyan and magenta constant.

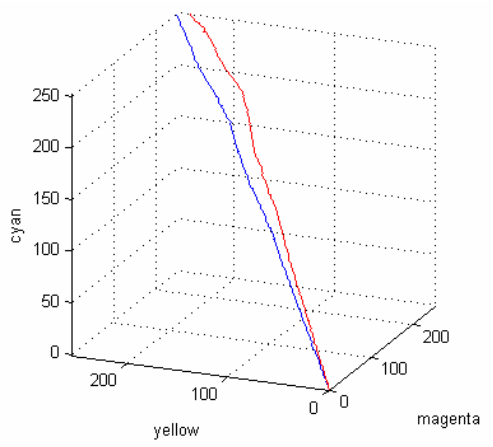


*Figure 3. TR001 (blue) vs TR004 (red) Neutral*

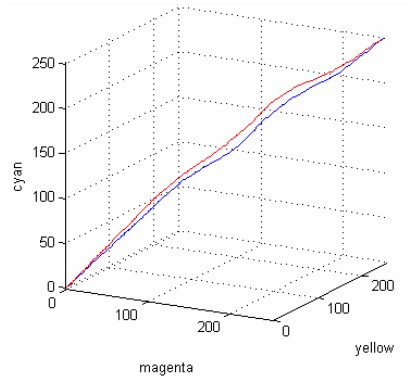


*Figure 4. TR001 (blue) vs TR004 (red) Neutral*

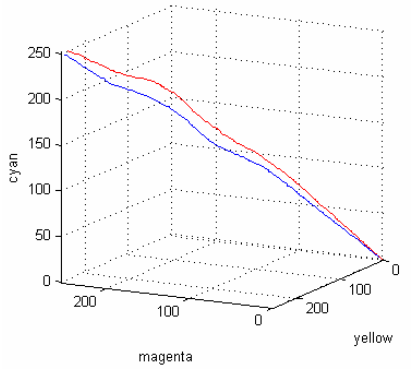


*Figure 5. TR001 (blue) vs TR004 (red) Neutral*

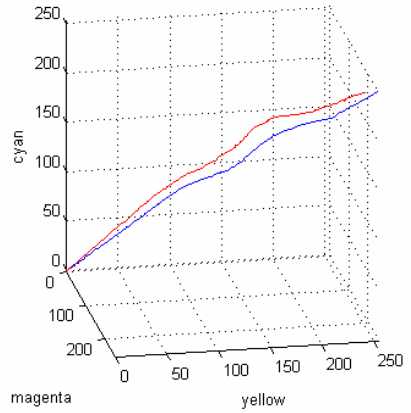


*Figure 6. TR001 (blue) vs TR004 (red) Neutral*

In constructing the above forced variations consideration was given to utilizing forcing large enough to substantially exceed the average model to measurement error insuring that model error was small in the outcome. Furthermore, forced variations larger than those variations reasonably allowing the approximation of linearity were disallowed.

Tables 3-5 provide the resultant forced variations (in increments of $\Delta L^* = 5$ beginning at $L^* = 95$ and decreasing) in cyan, magenta and yellow that were used to probe the printermodel for output functions for the TR001 neutral axis gain matrix estimation. In the below table the k record, for each entry, is zero.

**Table 3: Cyan Forcing Function (TR001)**

| c | m | y |
|---|---|---|
| 10.7 | 12.3 | 13.3 |
| 14.7 | 12.3 | 13.3 |
| 18.7 | 12.3 | 13.3 |
| 25.5 | 24.4 | 26.5 |
| 29.5 | 24.4 | 26.5 |
| 33.5 | 24.4 | 26.5 |
| 41.5 | 37.7 | 39.6 |
| 45.5 | 37.7 | 39.6 |
| 49.5 | 37.7 | 39.6 |
| 56.7 | 50.5 | 53.0 |
| 60.7 | 50.5 | 53.0 |
| 64.7 | 50.5 | 53.0 |
| 71.9 | 63.3 | 65.5 |
| 75.9 | 63.3 | 65.5 |
| 79.9 | 63.3 | 65.5 |
| 87.5 | 75.0 | 79.1 |
| 91.5 | 75.0 | 79.1 |
| 95.5 | 75.0 | 79.1 |
| 103.9 | 90.4 | 92.8 |
| 107.9 | 90.4 | 92.8 |
| 111.9 | 90.4 | 92.8 |
| 121.2 | 113.3 | 114.5 |
| 125.2 | 113.3 | 114.5 |
| 129.2 | 113.3 | 114.5 |
| 138.9 | 136.3 | 136.9 |
| 142.9 | 136.3 | 136.9 |
| 146.9 | 136.3 | 136.9 |
| 161.9 | 152.8 | 155.0 |
| 165.9 | 152.8 | 155.0 |
| 169.9 | 152.8 | 155.0 |
| 183.4 | 174.2 | 174.7 |
| 187.4 | 174.2 | 174.7 |
| 191.4 | 174.2 | 174.7 |
| 202.0 | 200.2 | 202.9 |
| 206.0 | 200.2 | 202.9 |
| 210.0 | 200.2 | 202.9 |
| 223.8 | 228.3 | 231.0 |
| 227.8 | 228.3 | 231.0 |
| 231.8 | 228.3 | 231.0 |
| 246.6 | 250.3 | 255.3 |
| 250.6 | 250.3 | 255.3 |
| 254.6 | 250.3 | 255.3 |

**Table 4: Magenta Forcing Function (TR001)**

| c | m | y |
|---|---|---|
| 14.7 | 8.3 | 13.3 |
| 14.7 | 12.3 | 13.3 |
| 14.7 | 16.3 | 13.3 |
| 29.5 | 20.4 | 26.5 |
| 29.5 | 24.4 | 26.5 |
| 29.5 | 28.4 | 26.5 |
| 45.5 | 33.7 | 39.6 |
| 45.5 | 37.7 | 39.6 |
| 45.5 | 41.7 | 39.6 |
| 60.7 | 46.5 | 53.0 |
| 60.7 | 50.5 | 53.0 |
| 60.7 | 54.5 | 53.0 |
| 75.9 | 59.3 | 65.5 |
| 75.9 | 63.3 | 65.5 |
| 75.9 | 67.3 | 65.5 |
| 91.5 | 71.0 | 79.1 |
| 91.5 | 75.0 | 79.1 |
| 91.5 | 79.0 | 79.1 |
| 107.9 | 86.4 | 92.8 |
| 107.9 | 90.4 | 92.8 |
| 107.9 | 94.4 | 92.8 |
| 125.2 | 109.3 | 114.5 |
| 125.2 | 113.3 | 114.5 |
| 125.2 | 117.3 | 114.5 |
| 142.9 | 132.3 | 136.9 |
| 142.9 | 136.3 | 136.9 |
| 142.9 | 140.3 | 136.9 |
| 165.9 | 148.8 | 155.0 |
| 165.9 | 152.8 | 155.0 |
| 165.9 | 156.8 | 155.0 |
| 187.4 | 170.2 | 174.7 |
| 187.4 | 174.2 | 174.7 |
| 187.4 | 178.2 | 174.7 |
| 206.0 | 196.2 | 202.9 |
| 206.0 | 200.2 | 202.9 |
| 206.0 | 204.2 | 202.9 |
| 227.8 | 224.3 | 231.0 |
| 227.8 | 228.3 | 231.0 |
| 227.8 | 232.3 | 231.0 |
| 250.6 | 246.3 | 255.3 |
| 250.6 | 250.3 | 255.3 |
| 250.6 | 254.3 | 255.3 |

**Table 5: Yellow Forcing Function (TR001)**

| c | m | y |
|---|---|---|
| 14.7 | 12.3 | 9.3 |
| 14.7 | 12.3 | 13.3 |
| 14.7 | 12.3 | 17.3 |
| 29.5 | 24.4 | 22.5 |
| 29.5 | 24.4 | 26.5 |
| 29.5 | 24.4 | 30.5 |
| 45.5 | 37.7 | 35.6 |
| 45.5 | 37.7 | 39.6 |
| 45.5 | 37.7 | 43.6 |
| 60.7 | 50.5 | 49.0 |
| 60.7 | 50.5 | 53.0 |
| 60.7 | 50.5 | 57.0 |
| 75.9 | 63.3 | 61.5 |
| 75.9 | 63.3 | 65.5 |
| 75.9 | 63.3 | 69.5 |
| 91.5 | 75.0 | 75.1 |
| 91.5 | 75.0 | 79.1 |
| 91.5 | 75.0 | 83.1 |
| 107.9 | 90.4 | 88.8 |
| 107.9 | 90.4 | 92.8 |
| 107.9 | 90.4 | 96.8 |
| 125.2 | 113.3 | 110.5 |
| 125.2 | 113.3 | 114.5 |
| 125.2 | 113.3 | 118.5 |
| 142.9 | 136.3 | 132.9 |
| 142.9 | 136.3 | 136.9 |
| 142.9 | 136.3 | 140.9 |
| 165.9 | 152.8 | 151.0 |
| 165.9 | 152.8 | 155.0 |
| 165.9 | 152.8 | 159.0 |
| 187.4 | 174.2 | 170.7 |
| 187.4 | 174.2 | 174.7 |
| 187.4 | 174.2 | 178.7 |
| 206.0 | 200.2 | 198.9 |
| 206.0 | 200.2 | 202.9 |
| 206.0 | 200.2 | 206.9 |
| 227.8 | 228.3 | 227.0 |
| 227.8 | 228.3 | 231.0 |
| 227.8 | 228.3 | 235.0 |
| 250.6 | 250.3 | 251.3 |
| 250.6 | 250.3 | 255.3 |
| 250.6 | 250.3 | 259.3 |

In the above tables, each separation is varied around a local point, holding all other separations constant thereby providing the forced input necessary to compute the partial derivatives in Eq. 1 for TR001.

**Table 6: Cyan Forcing Function (TR004)**

| c | m | y |
|---|---|---|
| 10.5 | 11.7 | 10.9 |
| 14.5 | 11.7 | 10.9 |
| 18.5 | 11.7 | 10.9 |
| 25.9 | 22.6 | 22.1 |
| 29.9 | 22.6 | 22.1 |
| 33.9 | 22.6 | 22.1 |
| 40.5 | 34.7 | 32.4 |
| 44.5 | 34.7 | 32.4 |
| 48.5 | 34.7 | 32.4 |
| 56.3 | 46.0 | 44.2 |
| 60.3 | 46.0 | 44.2 |
| 64.3 | 46.0 | 44.2 |
| 72.0 | 57.7 | 56.3 |
| 76.0 | 57.7 | 56.3 |
| 80.0 | 57.7 | 56.3 |
| 86.7 | 69.5 | 67.0 |
| 90.7 | 69.5 | 67.0 |
| 94.7 | 69.5 | 67.0 |
| 101.5 | 82.8 | 78.3 |
| 105.5 | 82.8 | 78.3 |
| 109.5 | 82.8 | 78.3 |
| 115.9 | 97.7 | 90.0 |
| 119.9 | 97.7 | 90.0 |
| 123.9 | 97.7 | 90.0 |
| 130.7 | 116.2 | 106.3 |
| 134.7 | 116.2 | 106.3 |
| 138.7 | 116.2 | 106.3 |
| 147.2 | 133.3 | 120.8 |
| 151.2 | 133.3 | 120.8 |
| 155.2 | 133.3 | 120.8 |
| 165.9 | 150.6 | 137.4 |
| 169.9 | 150.6 | 137.4 |
| 173.9 | 150.6 | 137.4 |
| 186.5 | 167.5 | 149.1 |
| 190.5 | 167.5 | 149.1 |
| 194.5 | 167.5 | 149.1 |
| 204.8 | 189.1 | 166.4 |
| 208.8 | 189.1 | 166.4 |
| 212.8 | 189.1 | 166.4 |
| 221.3 | 221.9 | 202.3 |
| 225.3 | 221.9 | 202.3 |
| 229.3 | 221.9 | 202.3 |
| 241.7 | 246.3 | 230.3 |
| 245.7 | 246.3 | 230.3 |
| 249.7 | 246.3 | 230.3 |

**Table 7: Magenta Forcing Function (TR004)**

| c | m | y |
|---|---|---|
| 14.5 | 7.7 | 10.9 |
| 14.5 | 11.7 | 10.9 |
| 14.5 | 15.7 | 10.9 |
| 29.9 | 18.6 | 22.1 |
| 29.9 | 22.6 | 22.1 |
| 29.9 | 26.6 | 22.1 |
| 44.5 | 30.7 | 32.4 |
| 44.5 | 34.7 | 32.4 |
| 44.5 | 38.7 | 32.4 |
| 60.3 | 42.0 | 44.2 |
| 60.3 | 46.0 | 44.2 |
| 60.3 | 50.0 | 44.2 |
| 76.0 | 53.7 | 56.3 |
| 76.0 | 57.7 | 56.3 |
| 76.0 | 61.7 | 56.3 |
| 90.7 | 65.5 | 67.0 |
| 90.7 | 69.5 | 67.0 |
| 90.7 | 73.5 | 67.0 |
| 105.5 | 78.8 | 78.3 |
| 105.5 | 82.8 | 78.3 |
| 105.5 | 86.8 | 78.3 |
| 119.9 | 93.7 | 90.0 |
| 119.9 | 97.7 | 90.0 |
| 119.9 | 101.7 | 90.0 |
| 134.7 | 112.2 | 106.3 |
| 134.7 | 116.2 | 106.3 |
| 134.7 | 120.2 | 106.3 |
| 151.2 | 129.3 | 120.8 |
| 151.2 | 133.3 | 120.8 |
| 151.2 | 137.3 | 120.8 |
| 169.9 | 146.6 | 137.4 |
| 169.9 | 150.6 | 137.4 |
| 169.9 | 154.6 | 137.4 |
| 190.5 | 163.5 | 149.1 |
| 190.5 | 167.5 | 149.1 |
| 190.5 | 171.5 | 149.1 |
| 208.8 | 185.1 | 166.4 |
| 208.8 | 189.1 | 166.4 |
| 208.8 | 193.1 | 166.4 |
| 225.3 | 217.9 | 202.3 |
| 225.3 | 221.9 | 202.3 |
| 225.3 | 225.9 | 202.3 |
| 245.7 | 242.3 | 230.3 |
| 245.7 | 246.3 | 230.3 |
| 245.7 | 250.3 | 230.3 |

**Table 8: Yellow Forcing Function (TR004)**

| c | m | y |
|---|---|---|
| 14.5 | 11.7 | 6.9 |
| 14.5 | 11.7 | 10.9 |
| 14.5 | 11.7 | 14.9 |
| 29.9 | 22.6 | 18.1 |
| 29.9 | 22.6 | 22.1 |
| 29.9 | 22.6 | 26.1 |
| 44.5 | 34.7 | 28.4 |
| 44.5 | 34.7 | 32.4 |
| 44.5 | 34.7 | 36.4 |
| 60.3 | 46.0 | 40.2 |
| 60.3 | 46.0 | 44.2 |
| 60.3 | 46.0 | 48.2 |
| 76.0 | 57.7 | 52.3 |
| 76.0 | 57.7 | 56.3 |
| 76.0 | 57.7 | 60.3 |
| 90.7 | 69.5 | 63.0 |
| 90.7 | 69.5 | 67.0 |
| 90.7 | 69.5 | 71.0 |
| 105.5 | 82.8 | 74.3 |
| 105.5 | 82.8 | 78.3 |
| 105.5 | 82.8 | 82.3 |
| 119.9 | 97.7 | 86.0 |
| 119.9 | 97.7 | 90.0 |
| 119.9 | 97.7 | 94.0 |
| 134.7 | 116.2 | 102.3 |
| 134.7 | 116.2 | 106.3 |
| 134.7 | 116.2 | 110.3 |
| 151.2 | 133.3 | 116.8 |
| 151.2 | 133.3 | 120.8 |
| 151.2 | 133.3 | 124.8 |
| 169.9 | 150.6 | 133.4 |
| 169.9 | 150.6 | 137.4 |
| 169.9 | 150.6 | 141.4 |
| 190.5 | 167.5 | 145.1 |
| 190.5 | 167.5 | 149.1 |
| 190.5 | 167.5 | 153.1 |
| 208.8 | 189.1 | 162.4 |
| 208.8 | 189.1 | 166.4 |
| 208.8 | 189.1 | 170.4 |
| 225.3 | 221.9 | 198.3 |
| 225.3 | 221.9 | 202.3 |
| 225.3 | 221.9 | 206.3 |
| 245.7 | 246.3 | 226.3 |
| 245.7 | 246.3 | 230.3 |
| 245.7 | 246.3 | 234.3 |

Tables 6-8 provides the resultant forced variations (in increments of $\Delta L^* = 5$ beginning at $L^* = 95$ and decreasing) in cyan, magenta and yellow that were used to probe the printermodel for output functions for the TR004 neutral axis gain matrix estimation. In the below table the k record, for each entry, is zero.

In the above tables, each separation is varied around a local point, holding all other separations constant thereby providing the forced input necessary to compute the partial derivatives in Eq. 1 for TR004.

## Output Forced Functions for Color Gain

Utilizing each of the input forcing functions defined in Tables 3-5, and the spectral Naugebauer printer model derived for each GATF source data set (TR001), the output functions associated with the input functions were computed for TR001.

Utilizing each of the input forcing functions defined in Tables 6-8, and the spectral Naugebauer printer model derived for each GATF source data set (TR004), the output functions associated with the input functions were computed for TR004.

**Table 9: Cyan Forced Function (TR001)**

| L* | a* | b* |
|---|---|---|
| 95.60 | 0.797 | 0.992 |
| 94.98 | -0.015 | 0.100 |
| 94.31 | -0.725 | -0.806 |
| 90.85 | 0.660 | 1.176 |
| 90.17 | -0.075 | 0.255 |
| 89.50 | -0.786 | -0.651 |
| 85.66 | 0.720 | 0.902 |
| 84.99 | 0.009 | -0.004 |
| 84.32 | -0.702 | -0.910 |
| 80.66 | 0.769 | 0.944 |
| 79.99 | 0.058 | 0.038 |
| 79.32 | -0.653 | -0.867 |
| 75.70 | 0.868 | 0.721 |
| 75.03 | 0.157 | -0.185 |
| 74.36 | -0.553 | -1.090 |
| 70.81 | 0.555 | 0.854 |
| 70.14 | -0.156 | -0.052 |
| 69.47 | -0.867 | -0.958 |
| 65.62 | 0.755 | 0.663 |
| 65.19 | -0.138 | -0.171 |
| 64.75 | -1.031 | -1.005 |
| 60.47 | 0.876 | 0.747 |
| 60.04 | -0.016 | -0.088 |
| 59.60 | -0.909 | -0.922 |
| 55.54 | 0.719 | 0.606 |
| 55.04 | 0.033 | -0.024 |
| 54.54 | -0.653 | -0.655 |
| 50.49 | 0.671 | 0.628 |
| 49.99 | -0.015 | -0.002 |
| 49.58 | -0.912 | -0.604 |
| 45.34 | 0.921 | 0.549 |
| 44.96 | -0.054 | -0.042 |
| 44.57 | -1.029 | -0.633 |
| 40.32 | 1.051 | 0.784 |
| 40.01 | -0.137 | 0.089 |
| 39.72 | -1.297 | -0.602 |
| 35.33 | 1.377 | 0.286 |
| 35.10 | 0.067 | -0.175 |
| 34.79 | -1.094 | -0.722 |
| 30.30 | 1.236 | 0.427 |
| 30.00 | 0.061 | -0.138 |
| 29.59 | -1.005 | -0.900 |

**Table 10: Magenta Forced Function (TR001)**

| L* | a* | b* |
|---|---|---|
| 95.64 | -1.154 | 0.447 |
| 94.98 | -0.015 | 0.100 |
| 94.24 | 1.131 | -0.108 |
| 90.83 | -1.214 | 0.602 |
| 90.17 | -0.075 | 0.255 |
| 89.50 | 1.043 | 0.027 |
| 85.64 | -1.130 | 0.343 |
| 84.99 | 0.009 | -0.004 |
| 84.31 | 1.125 | -0.218 |
| 80.65 | -1.081 | 0.386 |
| 79.99 | 0.058 | 0.038 |
| 79.32 | 1.180 | -0.211 |
| 75.69 | -0.982 | 0.163 |
| 75.03 | 0.157 | -0.185 |
| 74.35 | 1.277 | -0.420 |
| 70.79 | -1.295 | 0.295 |
| 70.14 | -0.156 | -0.052 |
| 69.48 | 0.983 | -0.399 |
| 65.84 | -1.277 | 0.176 |
| 65.19 | -0.138 | -0.171 |
| 64.51 | 0.983 | -0.417 |
| 60.50 | -1.039 | 0.334 |
| 60.04 | -0.016 | -0.088 |
| 59.55 | 0.944 | -0.275 |
| 55.51 | -0.990 | 0.397 |
| 55.04 | 0.033 | -0.024 |
| 54.56 | 1.048 | -0.165 |
| 50.49 | -1.261 | 0.243 |
| 49.99 | -0.015 | -0.002 |
| 49.50 | 1.109 | -0.192 |
| 45.39 | -1.102 | 0.399 |
| 44.96 | -0.054 | -0.042 |
| 44.42 | 1.071 | -0.210 |
| 40.38 | -1.167 | 0.539 |
| 40.01 | -0.137 | 0.089 |
| 39.63 | 0.881 | -0.298 |
| 35.55 | -1.074 | 0.339 |
| 35.10 | 0.067 | -0.175 |
| 34.53 | 1.308 | -0.698 |
| 30.42 | -0.995 | 0.297 |
| 30.00 | 0.061 | -0.138 |
| 29.46 | 1.226 | -0.770 |

**Table 11: Yellow Force Function (TR001)**

| L* | a* | b* |
|---|---|---|
| 95.05 | 0.218 | -1.089 |
| 94.98 | -0.015 | 0.100 |
| 94.88 | -0.217 | 1.519 |
| 90.26 | 0.169 | -1.005 |
| 90.17 | -0.075 | 0.255 |
| 90.08 | -0.316 | 1.649 |
| 85.07 | 0.251 | -1.249 |
| 84.99 | 0.009 | -0.004 |
| 84.89 | -0.256 | 1.375 |
| 80.07 | 0.306 | -1.243 |
| 79.99 | 0.058 | 0.038 |
| 79.89 | -0.207 | 1.417 |
| 75.11 | 0.403 | -1.452 |
| 75.03 | 0.157 | -0.185 |
| 74.93 | -0.108 | 1.194 |
| 70.24 | 0.109 | -1.431 |
| 70.14 | -0.156 | -0.052 |
| 70.04 | -0.421 | 1.327 |
| 65.27 | 0.110 | -1.449 |
| 65.19 | -0.138 | -0.171 |
| 65.09 | -0.418 | 1.172 |
| 60.07 | 0.321 | -0.901 |
| 60.04 | -0.016 | -0.088 |
| 59.98 | -0.416 | 0.960 |
| 55.07 | 0.338 | -0.779 |
| 55.04 | 0.033 | -0.024 |
| 55.01 | -0.243 | 1.004 |
| 50.03 | 0.138 | -0.975 |
| 49.99 | -0.015 | -0.002 |
| 49.96 | -0.291 | 1.026 |
| 45.01 | 0.204 | -0.669 |
| 44.96 | -0.054 | -0.042 |
| 44.80 | -0.236 | 0.858 |
| 40.03 | 0.198 | -0.646 |
| 40.01 | -0.137 | 0.089 |
| 39.99 | -0.458 | 0.891 |
| 35.16 | 0.071 | -1.084 |
| 35.10 | 0.067 | -0.175 |
| 35.02 | 0.118 | 0.875 |
| 30.10 | -0.001 | -1.200 |
| 30.00 | 0.061 | -0.138 |
| 29.99 | -0.193 | 0.493 |

**Table 12: Cyan Forced Function (TR004)**

| L* | a* | b* |
|---|---|---|
| 95.61 | 0.823 | 0.800 |
| 94.97 | 0.113 | 0.013 |
| 94.31 | -0.570 | -0.795 |
| 90.73 | 0.581 | 0.806 |
| 90.06 | -0.101 | -0.002 |
| 89.40 | -0.784 | -0.809 |
| 85.78 | 0.849 | 0.649 |
| 85.11 | 0.167 | -0.158 |
| 84.45 | -0.515 | -0.966 |
| 80.72 | 0.651 | 0.739 |
| 80.06 | -0.031 | -0.068 |
| 79.39 | -0.714 | -0.876 |
| 75.60 | 0.537 | 0.889 |
| 74.93 | -0.146 | 0.082 |
| 74.27 | -0.828 | -0.726 |
| 70.66 | 0.696 | 0.827 |
| 69.99 | 0.014 | 0.019 |
| 69.33 | -0.669 | -0.788 |
| 65.55 | 0.905 | 0.838 |
| 65.01 | -0.038 | -0.026 |
| 64.46 | -0.981 | -0.889 |
| 60.54 | 0.945 | 0.855 |
| 59.99 | 0.002 | -0.008 |
| 59.45 | -0.941 | -0.872 |
| 55.64 | 0.917 | 1.009 |
| 55.09 | -0.026 | 0.146 |
| 54.54 | -0.830 | -0.557 |
| 50.75 | 0.721 | 0.519 |
| 50.18 | 0.014 | -0.072 |
| 49.62 | -0.695 | -0.664 |
| 45.54 | 0.885 | 0.564 |
| 45.02 | 0.027 | 0.007 |
| 44.51 | -0.778 | -0.507 |
| 40.50 | 0.812 | 0.504 |
| 39.98 | 0.007 | -0.010 |
| 39.49 | -0.950 | -0.608 |
| 35.35 | 1.234 | 0.994 |
| 34.97 | -0.224 | 0.122 |
| 34.58 | -1.627 | -0.719 |
| 30.27 | 1.058 | 0.759 |
| 29.91 | -0.078 | 0.262 |
| 29.51 | -1.238 | -0.335 |
| 25.23 | 0.903 | 0.374 |
| 24.94 | -0.108 | -0.224 |
| 24.50 | -0.979 | -0.801 |

**Table 13: Magenta Forced Function (TR004)**

| L* | a* | b* |
|---|---|---|
| 95.70 | -1.020 | 0.319 |
| 94.97 | 0.113 | 0.013 |
| 94.19 | 1.237 | -0.108 |
| 90.78 | -1.237 | 0.321 |
| 90.06 | -0.101 | -0.002 |
| 89.31 | 1.005 | -0.100 |
| 85.85 | -0.954 | 0.052 |
| 85.11 | 0.167 | -0.158 |
| 84.36 | 1.274 | -0.257 |
| 80.79 | -1.156 | 0.173 |
| 80.06 | -0.031 | -0.068 |
| 79.30 | 1.076 | -0.167 |
| 75.66 | -1.273 | 0.345 |
| 74.93 | -0.146 | 0.082 |
| 74.18 | 0.961 | -0.017 |
| 70.73 | -1.105 | 0.211 |
| 69.99 | 0.014 | 0.019 |
| 69.24 | 1.120 | -0.079 |
| 65.76 | -1.144 | 0.073 |
| 65.01 | -0.038 | -0.026 |
| 64.25 | 1.069 | -0.124 |
| 60.69 | -1.075 | 0.098 |
| 59.99 | 0.002 | -0.008 |
| 59.42 | 1.020 | -0.127 |
| 55.66 | -1.044 | 0.265 |
| 55.09 | -0.026 | 0.146 |
| 54.52 | 0.992 | 0.026 |
| 50.75 | -1.004 | 0.047 |
| 50.18 | 0.014 | -0.072 |
| 49.61 | 1.060 | -0.195 |
| 45.58 | -1.104 | 0.141 |
| 45.02 | 0.027 | 0.007 |
| 44.47 | 1.157 | -0.128 |
| 40.54 | -1.149 | 0.096 |
| 39.98 | 0.007 | -0.010 |
| 39.40 | 1.304 | -0.157 |
| 35.56 | -1.515 | 0.272 |
| 34.97 | -0.224 | 0.122 |
| 34.41 | 1.016 | -0.056 |
| 30.41 | -1.191 | 0.541 |
| 29.91 | -0.078 | 0.262 |
| 29.41 | 1.036 | -0.051 |
| 25.43 | -1.286 | 0.047 |
| 24.94 | -0.108 | -0.224 |
| 24.29 | 1.208 | -0.493 |

**Table 14: Yellow Forced Function (TR004)**

| L* | a* | b* |
|---|---|---|
| 95.08 | 0.335 | -1.187 |
| 94.97 | 0.113 | 0.013 |
| 94.84 | -0.125 | 1.424 |
| 90.16 | 0.120 | -1.201 |
| 90.06 | -0.101 | -0.002 |
| 89.93 | -0.352 | 1.422 |
| 85.21 | 0.389 | -1.358 |
| 85.11 | 0.167 | -0.158 |
| 85.00 | -0.069 | 1.153 |
| 80.16 | 0.191 | -1.268 |
| 80.06 | -0.031 | -0.068 |
| 79.93 | -0.271 | 1.274 |
| 75.03 | 0.076 | -1.118 |
| 74.93 | -0.146 | 0.082 |
| 74.81 | -0.388 | 1.446 |
| 70.09 | 0.235 | -1.180 |
| 69.99 | 0.014 | 0.019 |
| 69.88 | -0.220 | 1.312 |
| 65.11 | 0.184 | -1.225 |
| 65.01 | -0.038 | -0.026 |
| 64.91 | -0.260 | 1.174 |
| 60.09 | 0.224 | -1.208 |
| 59.99 | 0.002 | -0.008 |
| 59.89 | -0.220 | 1.192 |
| 55.13 | 0.330 | -0.642 |
| 55.09 | -0.026 | 0.146 |
| 55.06 | -0.381 | 0.934 |
| 50.22 | 0.370 | -0.860 |
| 50.18 | 0.014 | -0.072 |
| 50.15 | -0.341 | 0.716 |
| 45.05 | 0.314 | -0.874 |
| 45.02 | 0.027 | 0.007 |
| 44.99 | -0.076 | 1.131 |
| 39.99 | 0.227 | -1.101 |
| 39.98 | 0.007 | -0.010 |
| 39.97 | -0.212 | 1.080 |
| 34.99 | -0.015 | -0.971 |
| 34.97 | -0.224 | 0.122 |
| 34.98 | -0.573 | 0.771 |
| 29.87 | 0.222 | -0.469 |
| 29.91 | -0.078 | 0.262 |
| 29.95 | -0.444 | 0.869 |
| 24.93 | 0.089 | -0.742 |
| 24.94 | -0.108 | -0.224 |
| 24.95 | -0.306 | 0.284 |

## Marking to Color Gain Matrix

The components of Equation 7, the color gain matrix, can now be derived for both TR001 and TR004 as a function of L* along the neutral axis. Computation of the elements of Eq. 7 was accomplished utilizing the forcing and forced tables with the central difference method for linearized equations[11].

*Note: Each gain matrix below, as a function of a local L*, is the transpose of the gain matrix represented in Eq. 7. Hence, in the tables below, the first column contains components in L*, the second column components in a* and the third column components in b*.*

Tables 15 and 16 enable assessment of any singular fluctuation in L*, a*, or b* for any singular fluctuation in marking c, m, y digital count.

**Table 15: Color Gain Matrices TR001 Neutral Axis**

| L* | Gain Components of Equation 1 | | |
|---|---|---|---|
| | -0.162 | -0.190 | -0.225 |
| 95 | -0.174 | 0.286 | -0.069 |
| | -0.021 | -0.054 | 0.326 |
| | -0.168 | -0.181 | -0.228 |
| 90 | -0.167 | 0.282 | -0.072 |
| | -0.023 | -0.061 | 0.332 |
| | -0.168 | -0.178 | -0.226 |
| 85 | -0.167 | 0.282 | -0.070 |
| | -0.023 | -0.063 | 0.328 |
| | -0.168 | -0.178 | -0.226 |
| 80 | -0.166 | 0.283 | -0.075 |
| | -0.023 | -0.064 | 0.333 |
| | -0.168 | -0.178 | -0.226 |
| 75 | -0.167 | 0.282 | -0.073 |
| | -0.023 | -0.064 | 0.331 |
| | -0.168 | -0.178 | -0.226 |
| 70 | -0.164 | 0.285 | -0.087 |
| | -0.025 | -0.066 | 0.345 |
| | -0.109 | -0.223 | -0.209 |
| 65 | -0.166 | 0.283 | -0.074 |
| | -0.023 | -0.066 | 0.328 |
| | -0.109 | -0.223 | -0.209 |
| 60 | -0.118 | 0.248 | -0.076 |
| | -0.011 | -0.092 | 0.233 |
| | -0.125 | -0.172 | -0.158 |
| 55 | -0.119 | 0.255 | -0.070 |
| | -0.008 | -0.073 | 0.223 |
| | -0.114 | -0.198 | -0.154 |
| 50 | -0.123 | 0.296 | -0.054 |
| | -0.009 | -0.054 | 0.250 |
| | -0.096 | -0.244 | -0.148 |
| 45 | -0.121 | 0.272 | -0.076 |
| | -0.026 | -0.055 | 0.191 |
| | -0.075 | -0.293 | -0.173 |
| 40 | -0.093 | 0.256 | -0.105 |
| | -0.004 | -0.082 | 0.192 |
| | -0.067 | -0.309 | -0.126 |
| 35 | -0.128 | 0.298 | -0.130 |
| | -0.017 | 0.006 | 0.245 |
| | -0.089 | -0.280 | -0.166 |
| 30 | -0.121 | 0.278 | -0.133 |
| | -0.014 | -0.024 | 0.212 |
| | -0.162 | -0.190 | -0.225 |

**Table 16: Color Gain Matrices TR004 Neutral Axis**

| L* | Gain Components of Equation 1 | | |
|---|---|---|---|
| | -0.162 | -0.174 | -0.199 |
| 95 | -0.188 | 0.282 | -0.053 |
| | -0.029 | -0.057 | 0.326 |
| | -0.166 | -0.171 | -0.202 |
| 90 | -0.184 | 0.280 | -0.053 |
| | -0.030 | -0.059 | 0.328 |
| | -0.166 | -0.171 | -0.202 |
| 85 | -0.187 | 0.278 | -0.039 |
| | -0.027 | -0.057 | 0.314 |
| | -0.166 | -0.171 | -0.202 |
| 80 | -0.186 | 0.279 | -0.042 |
| | -0.028 | -0.058 | 0.318 |
| | -0.166 | -0.171 | -0.202 |
| 75 | -0.186 | 0.279 | -0.045 |
| | -0.028 | -0.058 | 0.320 |
| | -0.166 | -0.171 | -0.202 |
| 70 | -0.187 | 0.278 | -0.036 |
| | -0.027 | -0.057 | 0.311 |
| | -0.137 | -0.236 | -0.216 |
| 65 | -0.189 | 0.277 | -0.025 |
| | -0.025 | -0.055 | 0.300 |
| | -0.137 | -0.236 | -0.216 |
| 60 | -0.158 | 0.262 | -0.028 |
| | -0.025 | -0.055 | 0.300 |
| | -0.138 | -0.218 | -0.196 |
| 55 | -0.143 | 0.255 | -0.030 |
| | -0.009 | -0.089 | 0.197 |
| | -0.141 | -0.177 | -0.148 |
| 50 | -0.143 | 0.258 | -0.030 |
| | -0.009 | -0.089 | 0.197 |
| | -0.129 | -0.208 | -0.134 |
| 45 | -0.139 | 0.283 | -0.034 |
| | -0.008 | -0.049 | 0.251 |
| | -0.126 | -0.220 | -0.139 |
| 40 | -0.143 | 0.307 | -0.032 |
| | -0.002 | -0.055 | 0.273 |
| | -0.096 | -0.358 | -0.214 |
| 35 | -0.143 | 0.316 | -0.041 |
| | -0.001 | -0.070 | 0.218 |
| | -0.095 | -0.287 | -0.137 |
| 30 | -0.125 | 0.278 | -0.074 |
| | 0.010 | -0.083 | 0.167 |
| | -0.092 | -0.235 | -0.147 |
| 25 | -0.142 | 0.312 | -0.067 |
| | 0.002 | -0.049 | 0.128 |
| | -0.162 | -0.174 | -0.199 |

**Table 17: Color Gain Matrix for TR004 Neutral at L* = 95 (Highlights)**

| | | | | |
|---|---|---|---|---|
| $\begin{bmatrix} \frac{\partial L^*}{\partial c} & \frac{\partial L^*}{\partial m} & \frac{\partial L^*}{\partial y} \\ \frac{\partial a^*}{\partial c} & \frac{\partial a^*}{\partial m} & \frac{\partial a^*}{\partial y} \\ \frac{\partial b^*}{\partial c} & \frac{\partial b^*}{\partial m} & \frac{\partial b^*}{\partial y} \end{bmatrix}$ | = | -0.162 | -0.188 | -0.029 |
| | | -0.174 | 0.282 | -0.057 |
| | | -0.199 | -0.053 | 0.326 |

## Example: Constant, Simultaneous Forcing of c,m,y Separations by 1%

Separate analysis indicates that the uncertainty associated with marking laydown is 1% for all separations. For the TR004 data set at an L* of 95 the Color Gain Matrix is (from Table 16) (and transposing the numbers in that table according the note preceding that table):

Table 17 enables the rapid and simple visualization of the magnitude and structure of color variability in the presence of marking variation. The primary drivers for variation in L* are cyan and magenta. Yellow, as shown in the above table, plays little role in L* variability. Similarly the primary driver for variation in a* is magenta, with cyan playing a secondary role and yellow playing only a small role (row 2 above). Lastly, the primary driver for b* variation is yellow, with cyan as a secondary driver and magenta offering little by way of color gain (row 3).

Rapid visualization of the color variability structure is shown in Figure 7.

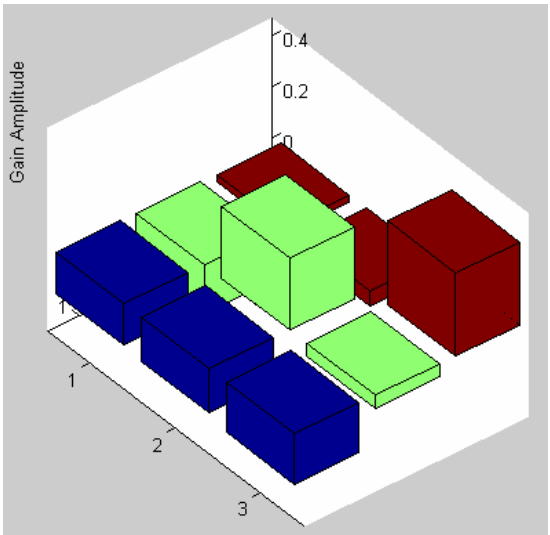


*Figure 7. Gain Amplitude vs Matrix Dimension Visualization.*

The ability to rapidly sort through expected amplitude of variation as a function of separation for each color dimension is valuable in a variety of ways.

## Example

### *Correlated (in c,m,y) vs Uncorrelated (in c,m,y) Euclidean Color Error from Color Gain Singular Variation in L*, a*, and b.*

A significant result, to be illustrated, is the observation that total color variation, along the neutral axis, resultant from correlated variations in c,m,y is smaller than total color variation resultant from uncorrelated variation in c,m,y. For many natural processes this is a counterintuitive result. To initiate a look at this interesting finding L* is first considered as a function of correlated and uncorrelated fluctuations in c,m,y.

### *Error in L**

Using the gain matrix of Table 17 the correlated color error associated with the singular component of color, L*, is computed, for a 1% correlated fluctuation in c, m, y, as:

(from Eq. 8).

$$dL^*_{cmy\_correlated} = \text{sqrt}[\ ((-0.162 - 0.188 - 0.029)*2.55)^2\ ]$$

$$\Delta L^*_{cmy\_correlated} = 0.96.$$

Likewise, for c,m,y fluctuations which are uncorrelated Eq. 12 applies.

$$dL^*_{cmy\_uncorrelated} = \text{sqrt}[(-2.55 * 0.162)^2 + (-2.55 * 0.188)^2 + (-2.55 * 0.029)^2]$$

$$dE_{L^*\ cmy\_uncorrelated} = 0.63.$$

Uncorrelated fluctuations (in c,m,y) result in reduced L* variation relative to correlated fluctuations. This is a singular result of the fact that L* variation, for all three separations, moves in the same direction for variation in any of the three separations.

### *Error in a**

Using the gain matrix of Table 17, the correlated color error associated with the singular component of color, a*, is computed, for a 1% correlated fluctuation in c,m,y as:

(from Eq. 9).

$da^*_{cmy\_correlated} = sqrt[(2.55*(-0.174+0.282-0.057))^2]$

$\Delta a^*_{cmy\_correlated} = 0.28$

Likewise, for c,m,y fluctuations which are uncorrelated Eq. 13 applies.

$da^*_{cmy\_uncorrelated} = sqrt[(2.55*-0.174)^2 + (2.55*0.282)^2 + (2.55*-0.057)^2]$

$dE_{a*cmy\_uncorrelated} = 0.85$

### *Error in b**

Using the gain matrix of Table 17, the correlated color error associated with the singular component of color, a*, is computed, for a 1% correlated fluctuation in c,m,y as:

(from Eq. 10).

$db^*_{cmy\_correlated} = sqrt[(2.55*(-0.199 - 0.053 + 0.326))^2]$;

$\Delta b^*_{cmy\_correlated} = 0.19$

Likewise, for c,m,y fluctuations which are uncorrelated Eq. 14 applies.

$db*cmy\_uncorrelated = sqrt((2.55*-0.199)^2 + (2.55*-0.053)^2 + (2.55*0.326)^2)$

$dE_{b*cmy\_uncorrelated} = 0.98$

Correlated error, while larger relative to uncorrelated error for L*, reverses when considering the color components a* and b*. In both the case of a* and b* correlation in c,m,y fluctuation results in forcing internal components of a* and b* in opposing directions. Internal cancellation during correlated fluctuation results in reduced error for the a* and b* components of the color space L*a*b*.

The preceding result can be shown to hold for all color gain matrices along neutral for the presses considered in this paper.

## Example:

### *Correlated (in c,m,y) vs Uncorrelated (in c,m,y) Euclidean Color Error from Color Gain*

#### *Cumulative Error in L*,a*, and b**

Next we extend the example of Table 17 to cumulative color error, in all three dimensions, via equations 11 and 15. For an uncertainty of 1% in separation laydown (all separations) the correlated (in c,m,y) color error is (from Eq. 11):

$sqrt\ \{[\ (-0.162 - 0.188 - 0.029)*2.55]^2$

$\Delta E_{cmy\_correlated} = +\ [\ (-0.174 + 0.282 - 0.057)*2.55]^2$

$+\ [\ (-0.199 - 0.053 + 0.326)*2.55]^2\}$

$\Delta E_{cmy\_correlated} = 0.992$

Hence, the correlated (in c,m,y) error for a 1% uncertainty in each separation laydown could be expected. In other words, print to print variability, in this region of neutral, for a known uncertainty of 1%, would result in a correlated Euclidean Delta E of 0.992.

For an uncertainty of 1% in separation laydown (all separations) the correlated (in c,m,y) color error is (from Eq. 15):

$sqrt\{[\ (c*0.162)^2 + (c*0.174)^2 + (c*0.199)^2]$

$\Delta E_{cmy\_uncorrelated} = +\ [\ (c*0.188)^2 + (c*0.282)^2 + (c*0.053)^2]$

$+\ [\ (c*0.029)^2 + (c*0.057)^2 + (c*0.0326)^2]\}$

where c is the digital count uncertainty of 2.55.

$\Delta E_{cmy\_uncorrelated} = 1.45$

Correlated error is, in the cumulative case of L*a*b*, smaller than uncorrelated error.

These results are of interest when compared to many natural processes, and certainly process plant processes, where internal fluctuations have typically positive variation. In that case, the correlated error is larger than uncorrelated error. Indeed, this is the normal case encountered in statistical sampling outcomes.

## Composite, Correlated and Uncorrelated Color Error vs L* Along Neutral

### *Constant, Simultaneous 1% Uncertainty in c,m,y*

It is of interest to estimate the overall output fluctuation in color, as a function of L*, when a 1% uncertainty exists in the marking laydown of all separations of 8 bit printing.

This estimate is presented, as a function of L*, along the neutral axes in Tables 17 and 18.

**Table 17: Uncorrelated and Correlated Error**

| Uncertainty in c,m,y = 1%<br>TR001 | | |
|---|---|---|
| **L*** | **Uncorrelated** | **Correlated** |
| 95 | 1.485 | 0.919 |
| 90 | 1.487 | 0.920 |
| 85 | 1.477 | 0.920 |
| 80 | 1.485 | 0.920 |
| 75 | 1.482 | 0.920 |
| 70 | 1.510 | 0.920 |
| 65 | 1.466 | 0.769 |
| 60 | 1.273 | 0.645 |
| 55 | 1.165 | 0.642 |
| 50 | 1.268 | 0.647 |
| 45 | 1.209 | 0.628 |
| 40 | 1.276 | 0.577 |
| 35 | 1.392 | 0.541 |
| 30 | 1.322 | 0.616 |

**Table 18: Uncorrelated and Correlated Error**

| Uncertainty in c,m,y = 1%<br>TR004 | | |
|---|---|---|
| **L*** | **Uncorrelated** | **Correlated** |
| 95 | 1.454 | 0.995 |
| 90 | 1.453 | 0.995 |
| 85 | 1.429 | 0.995 |
| 80 | 1.435 | 0.995 |
| 75 | 1.440 | 0.995 |
| 70 | 1.425 | 0.995 |
| 65 | 1.459 | 0.907 |
| 60 | 1.417 | 0.831 |
| 55 | 1.244 | 0.755 |
| 50 | 1.162 | 0.748 |
| 45 | 1.258 | 0.737 |
| 40 | 1.341 | 0.744 |
| 35 | 1.525 | 0.682 |
| 30 | 1.259 | 0.594 |
| 25 | 1.213 | 0.633 |

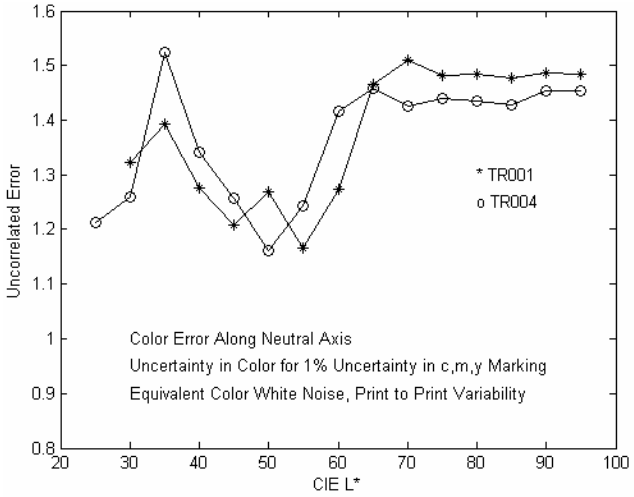


*Figure 8. Uncorrelated Color Error for 1% Uncertainty in c,m,y.*

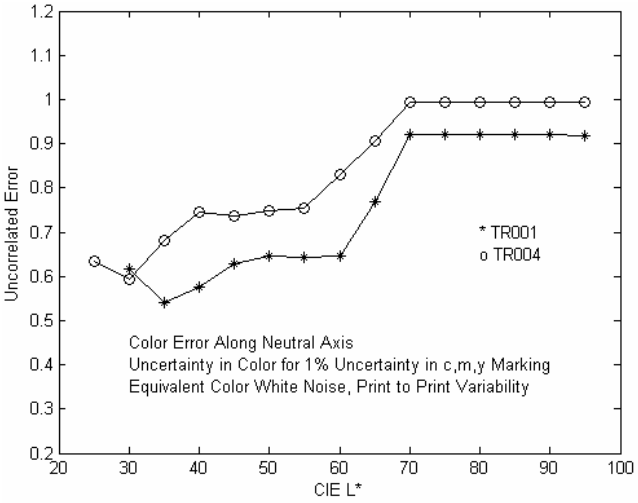


*Figure 9. Correlated Color Error for 1% Uncertainty in c,m,y.*

Uncorrelated and correlated color error, for an uncertainty in c,m,y laydown of 1%, are plotted in the below Figures 8 and 9 as a function of distance in L* along the neutral axis.

For the uncorrelated case, the magnitude of color error ranges between 1.2 and 1.6 $\Delta E_{ab}$. A minimum in color variation for forced variations in c,m,y occurs near L* of 50. The highlight and high midtone regions offer the most variation. However, at L* of 30 for both TR001 and TR004 there is a minor peak in color error.

For the case of correlation in c,m,y, the magnitude of color error ranges from 0.5 to 1 DE. This error is substantially less than the uncorrelated (in c,m,y) case. As previously noted, the reduced error resultant from simultaneous forcing of c,m,y corresponds to the generation of color error vectors with different, and opposing, direction. The uncorrelated case does not consider direction of forced outcome, hence, the larger error. For correlated color error, the highlight region offers the most fluctuation in color for simultaneous forced variations in c,m,y. The dark, neutral region where c, m, y laydown is most results in the least variation (a constant % fluctuation has least impact for the larger c,m,y numbers).

## Conclusions and Discussion

Print to print variability, both within run, and across runs, is critical in print shops where signed proofs drive profitability. This paper offers a method, derived from variational principles, along the critical neutral axis, of estimating color variation in the presence of known forced variation in separation laydown.

Local variational methods via model linearization, common in the estimation of point stability in process control systems, have been developed and applied to the TR001 and TR004 data set. These linearization methods enable the estimation of local variability in color in the presence of forced variations in marking.

Results indicate that, for reasonable estimates of forced variation in c,m,y laydown (1%) that print to print variability (that variation forced through Eq. 1) range between 0.5 and 1.6 Delta E depending on correlation between the separations. CGATS has reported print variability results for their TR004 data set as an average of 0.26 $\Delta E_{ab}$[12]. CGATS results are for ALL colors of the IT8 data set. Those colors for which only one, or two separations contribute to color formation would be expected to vary less than those formed along neutral. Hence, results in this paper form a reasonable upper bound for near neutral offset printer, print to print variability.

Results also indicate substantial difference in error when c,m,y are considered correlated or uncorrelated. Error is reduced for the case where perfect correlation is considered since forcing c,m,y in the same direction force color in opposing directions thereby reducing error.

For constant forcing of c,m,y, the minimum error occurs for midtones in the case of uncorrelated error and for dark neutrals in the case of correlated error. In both correlated and uncorrelated the highlights offer the most variation for constant, forced c,m,y variations.

Future work may include variational results around all IT8 data and subsequent tuning for forced variation to match experimental data thereby elucidating the random fluctuations associated with marking. Additionally, the extraction of the actual forcing function (in c,m,y) as a function of tone reproduction would be a worthwhile effort.

## Appendix A

### *TR001 Model Data Compared with Specification Data (L*a*b* in ΔEab space)*

A comparison of all IT8 data yield the following histogram based on printermodel methods described by Balasubramanian.[10]

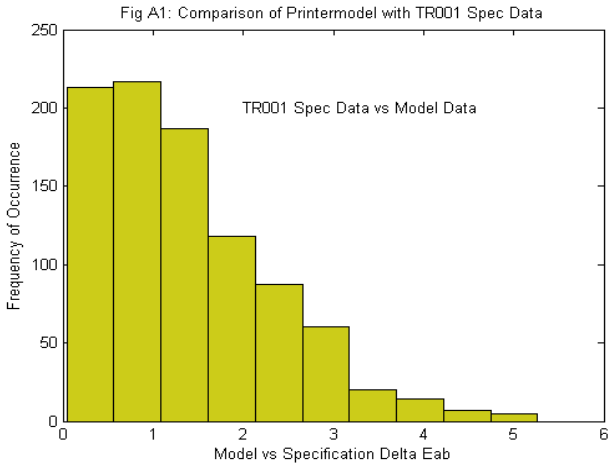


*Figure A1. Comparison of Printermodel with TR001 Spec Data*

## References


1. Seborg, Dale E., Edgar, Thomas F., Mellichamp, Duncan A.: "Process Dynamics and Control", 2004, John Wiley and Sons, Inc..
2. Rao, Guthikonda V.: "Complex Digital Control Systems", 1979, Von Nostrand Reinhold Co.
3. Coughanowr, Donald R., Koppel, Lowell B.: "Process Systems Analysis and Control", McGraw-Hill Book Company, 1965.
4. Giorgianni, Edward J., Madden, Thomas E.: "Digital Color Management: Encoding Solutions", 1998, Addison-Wesley Company.
5. Yule, Y.A.C.: "Principles of Color Reproduction", p. 84, 1967, John Wiley and Sons.
5. Hunt, R.W.G, "The Reproduction of Color", Fourth Edition, 1987, p. 66, Fountain Press, England.
6. Wyszecki, G., and Stiles, W.S.: "Color Science: Concepts and Methods, Quantitative Data and Formulae", p. 166, Second Edition, 2000, John Wiley and Sons.
7. Coughanowr, Donald R., Koppel, Lowell B.: "Process Systems Analysis and Control", McGraw-Hill Book Company, p. 331, 1965.
8. Luo, M. R., Rigg, Cui, B.: "*The Development of the CIE 2000 Colour Difference Formula, CIEDE2000*", Color Research and Application, p 340., Oct. 2001.
9. Balasubramanian, Raja: "*Optimization of the spectral Neugebauer model for printer characterization*", Journal of Electronic Imaging, p 156, April 1999.
10. James, M.L, Smith, G.M., Wolford, J.C.: "Applied Numerical Methods for Digital Computation", Second Edition, p. 346, Harper and Row Publishers, 1977.
11. CGATS DTR 004-2003: "*A CGATS Draft Technical Report for Trial Use*", 2003.


## Author Biography

*Dr. Michael Sanchez began his imaging work in the black and white darkroom of Elkhart High School. Upon completing a Ph.D. in Chemical Engineering at the University of Texas in 1987, and due in large part to his enthusiasm for photography, he sought and obtained, a position with the venerable Eastman Kodak Company. After several years working in process control to minimize flucutations in final coated film color output (daytime job) and working in the free Kodak color darkrooms (night job) he entered the RIT program in Imaging Science - Color Track. There he met Mark Fairchild and became fascinated with the Helmholtz-Kolhrausch effect via a paper previously published by Fairchild and Pirrotta. Two years later he completed his M.S. with a report on the H-K effect. The depth of the issues presented by that one effect still occupy his time and mind. Sanchez currently works at Xerox corporation where he is Senior Color Scientist for the DocuSP high speed color controller team. Sanchez maintains an ardent love of all things imaging, having more recently entered the video world.*